The R″ wave in V1 and the negative terminal QRS vector in aVF combine to a novel 12-lead ECG algorithm to identify slow conducting anatomical isthmus 3 in patients with tetralogy of Fallot

Justin Wallet [1,2,3], Yoshitaka Kimura [1,2,3], Nico A. Blom [3,4],
Sumche Man [1,2,3], Monique R.M. Jongbloed [1,3,5], and Katja Zeppenfeld [1,2,3]*

[1]Department of Cardiology, Heart Lung Centre, Leiden University Medical Centre, P.O. Box 9600, 2300 RC Leiden, The Netherlands; [2]Willem Einthoven Centre of Arrhythmia Research and Management (WECAM), Leiden, The Netherlands; [3]Centre for Congenital Heart Disease Amsterdam-Leiden (CAHAL), Leiden, The Netherlands; [4]Department of Paediatric Cardiology, Leiden University Medical Centre, Leiden, The Netherlands; and [5]Department of Anatomy & Embryology, Leiden University Medical Centre, Leiden, The Netherlands

Aims	Patients with repaired tetralogy of Fallot (rTOF) have an increased risk of ventricular tachycardia (VT), with slow conducting anatomical isthmus (SCAI) 3 as dominant VT substrate. In patients with right bundle branch block (RBBB), SCAI 3 leads to local activation delay with a shift of terminal RV activation towards the lateral RV outflow tract which may be detected by terminal QRS vector changes on sinus rhythm electrocardiogram (ECG).
Methods and results	Consecutive rTOF patients aged ≥16 years with RBBB who underwent electroanatomical mapping at our institution between 2017–2022 and 2010–2016 comprised the derivation and validation cohort, respectively. Forty-six patients were included in the derivation cohort (aged 40±15 years, QRS duration 165±23 ms). Among patients with SCAI 3 (*n* = 31, 67%), 17 (55%) had an R″ in V1, 18 (58%) had a negative terminal QRS portion (NTP) ≥80 ms in aVF, and 12 (39%) had both ECG characteristics, compared to only 1 (7%), 1 (7%), and 0 patient without SCAI, respectively. Combining R″ in V1 and/or NTP ≥80 ms in aVF into a diagnostic algorithm resulted in a sensitivity of 74% and specificity of 87% in detecting SCAI 3. The inter-observer agreement for the diagnostic algorithm was 0.875. In the validation cohort [*n* = 33, 18 (55%) with SCAI 3], the diagnostic algorithm had a sensitivity of 83% and specificity of 80% for identifying SCAI 3.
Conclusion	A sinus rhythm ECG-based algorithm including R″ in V1 and/or NTP ≥80 ms in aVF can identify rTOF patients with a SCAI 3 and may contribute to non-invasive risk stratification for VT.

Graphical Abstract

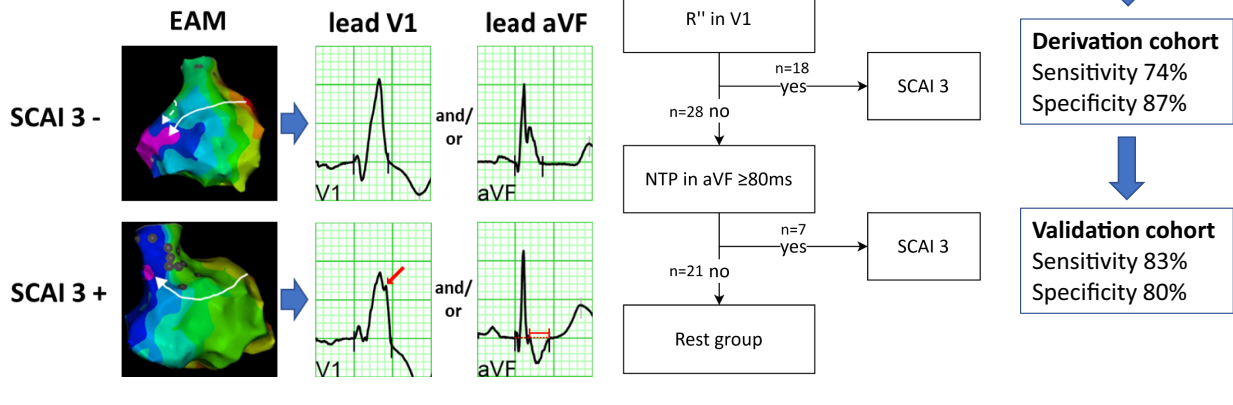**12-lead ECG diagnostic algorithm for SCAI 3 in tetralogy of Fallot**

Aim
To assess if terminal vector orientation on the 12-lead ECG can detect slow conducting anatomical isthmus 3 in patients with repaired tetralogy of Fallot, aged ≥16 years with RBBB in sinus rhythm.

2017-2022 Derivation cohort (n=46)
2010-2016 Validation cohort (n=33)

Results
R'' in lead V1 and **negative terminal portion of the QRS complex (NTP) ≥80ms in lead aVF** independently predictive of SCAI 3.

EAM   lead V1   lead aVF

SCAI 3 -   and/or
              V1   aVF

SCAI 3 +   and/or
              V1   aVF

Derivation cohort

All patients
n=46

R'' in V1
              n=18 yes → SCAI 3
n=28 no

NTP in aVF ≥80ms
              n=7 yes → SCAI 3
n=21 no

Rest group

Derivation cohort
Sensitivity 74%
Specificity 87%

Validation cohort
Sensitivity 83%
Specificity 80%

Keywords   Tetralogy of Fallot • Congenital heart disease • Electroanatomical mapping • Ventricular tachycardia • Non-invasive risk stratification • Electrocardiography

What's new?

- In patients repaired for tetralogy of Fallot, the most prevalent ventricular tachycardia (VT) substrate, slow conducting anatomical isthmus (SCAI) 3, causes a shift of the terminal right ventricular activation towards the lateral right ventricular outflow tract, which can be detected on the 12-lead ECG as a terminal vector with rightward and superior direction.
- A diagnostic algorithm is provided that uses the ECG parameters R'' in lead V1 and/or duration of the negative terminal portion of the QRS complex ≥80 ms in lead aVF, resulting in a sensitivity of 74% and specificity of 87% in detecting SCAI 3, with a high inter-observer agreement.
- In a validation cohort, similar high sensitivity and specificity for the algorithm could be confirmed.
- This promising and easy-to-use new diagnostic algorithm may contribute to non-invasive detection of VT substrates and risk stratification in patients with tetralogy of Fallot.

Introduction

Advances in surgical repair and medical treatment have improved survival in patients with tetralogy of Fallot (TOF). While fewer patients die from perioperative events and early heart failure, the risk of sudden cardiac death (SCD) due to sustained monomorphic ventricular tachycardia (SMVT) remains of concern.[1–10] The vast majority of documented ventricular tachycardia (VT) is due to re-entry and the critical component of the circuit is typically located within anatomically defined isthmuses (AI) bordered by unexcitable structures such as surgical scars, patches, and valve annuli.[8,11] Electroanatomical mapping (EAM) studies could demonstrate that VT-related AI have slow conducting properties already during sinus rhythm (SR). Indeed, in patients with spontaneous and/or induced SMVT, slow conducting anatomical isthmuses (SCAIs) were confirmed in 93%, with SCAI 3, located at the infundibular septum between the ventricular septal defect (VSD) patch and pulmonary annulus, as most prevalent VT substrate.[8]

In TOF patients and a right bundle branch block (RBBB) pattern, initial activation of the right ventricle (RV) during SR is similar compared to subjects with structurally normal hearts with RBBB.[12–14] Regardless of the level of block of a post-operative RBBB pattern, the basal lateral RV is usually activated late.[14,15] Localized septal infundibular activation delay results, however, in a shift of the latest activation from the basal lateral RV towards the lateral RV outflow tract (RVOT).[12]

We hypothesize that this rightward and superiorly directed terminal activation of the RV may influence the terminal portion of the QRS vector on a 12-lead electrocardiogram (ECG) during SR. The aim of the study was to evaluate whether specific characteristics of the terminal portion of the QRS vector can non-invasively identify repaired tetralogy of Fallot (rTOF) patients with SCAI 3.

Methods

Study population and study design

The study population consisted of all consecutive patients with repaired TOF referred for EAM and programmed electrical stimulation (PES) from 2010 to 2022 to the Leiden University Medical Centre (LUMC), Leiden,

the Netherlands. Patients were referred for EAM/PES for the following indications: (1) treatment of spontaneous ventricular arrhythmias (VA), (2) before pulmonary valve replacement (PVR), or (3) risk stratification for VA. Patients in the risk stratification group were referred because of the presence of previously reported, non-invasively assessed risk factors for VT/SCD [e.g. palliative shunt, transventricular and/or late repair, cardiac syncope, QRS duration ≥180 ms, non-sustained VT, depressed left ventricular (LV) or RV function, extensive LV/RV late gadolinium enhancement (LGE) on cardiac magnetic resonance imaging (CMR)].[1,16–19] Patients provided informed consent before the procedure.

Patients were assigned to the algorithm derivation or validation cohort according to the timing of EAM/PES. Patients evaluated between January 2017 and December 2022 were assigned to the derivation cohort and patients evaluated between January 2010 and December 2016 to the validation cohort. All patients were included and underwent EAM/PES according to the same clinical protocol implemented in 2005.[8] The more recent cohort was used to derive the algorithm only for practical reasons, as EAM data were more easily retrievable from the data storing system.

Patients eligible for inclusion were those with an RBBB pattern (QRS width ≥120 ms), age ≥16 years at time of procedure, with a non-ventricular-paced 12-lead ECG. Patients with persistent atrial fibrillation or atrial flutter, patients with known other VT substrates not related to AI, and patients with AI 4 were excluded from analysis of the ECG parameters and SCAI 3.

This study was approved by the internal review board of the cardiology and paediatric cardiology department of the LUMC. The Medical Ethics Committee Leiden The Hague Delft (GP21.137) waived the need for written informed consent.

Electroanatomical mapping and programmed electrical stimulation

Three-dimensional EAM and PES were performed under conscious sedation or general anaesthesia, where appropriate. The PES protocol consisted of up to four drive-cycle lengths (CL; 600, 500, 400, and 350 ms) with up to four extra stimuli, until the ventricular effective refractory period or a minimum CL of 200 ms (180 ms in paediatric patients) was reached. PES was performed from the RV apex and at the infundibulum close to AI 3 and was repeated during isoproterenol infusion if VT was not inducible at baseline. High-density voltage and activation mapping was performed during baseline rhythm using the CARTO™ system and the ThermoCool® ablation catheter (Biosense Webster Inc., Irvine, CA). In low-voltage areas (bipolar voltage <1.5 mV), absence of ventricular capture following high output pacing (10 mA/2 ms) indicated areas of dense scar, valve tissue, or artificial material [e.g. VSD patch or transannular patch (TAP)]. These non-excitable areas form the fixed boundaries of the four previously described anatomical isthmuses (AIs), namely: AI 1, located between TAP/RV incision and tricuspid annulus; AI 2, between non-transannular RVOT patch/RV incision and pulmonary annulus; AI 3, between VSD patch and pulmonary annulus; and AI 4, between VSD patch and tricuspid annulus.[8,11] Conduction velocity (CV) across the AI was determined as previously described.[8,12] Briefly, the AI length was measured as the distance between the first normal bipolar electrograms (voltage >1.5 mV) at each side of the isthmus. AI conduction time was calculated as the difference in local activation times (rapid negative deflection of the unipolar signal) at these points and the CV by dividing distance by conduction time. A slow conducting AI (SCAI) was defined as CV <0.5 m/s and a blocked AI, if no conduction through AI 3 could be detected. As a SCAI and blocked AI 3 similarly affect the terminal RV activation they were combined to SCAI 3.

In patients with SCAI, radiofrequency catheter ablation (RFCA) or surgical cryoablation concomitant with PVR was performed to transect the SCAI by connecting the unexcitable boundaries. Endpoints of ablation were bidirectional block across the ablation line and additionally, in patients who underwent RFCA, non-inducibility of VT.

Baseline characteristics

Details on surgical history, clinical characteristics, and imaging modalities (echocardiography, CMR) were collected from electronic health and surgical records. The 12-lead ECG recorded prior to EAM/PES was selected for analysis. In case of severe baseline drift, artefacts, paroxysmal atrial arrhythmias, frequent premature ventricular contractions, or incidental ventricular pacing, an earlier recorded ECG was used.

ECG analysis

For comprehensive analysis of the ECG, *Leiden ECG Analysis and Decomposition Software* (LEADS) was employed.[20,21] Raw electrocardiographic data, consisting of 8-channel recordings of 10 s ECGs in comma-separated value files, were inserted into this MATLAB program (The Mathworks Inc., Natick, MA, version: 2007b). With LEADS, the QRS complexes and T waves are automatically detected in the spatial velocity signal and the program proposes selected beats for averaging based on minimization of baseline drifts and artefacts, which can afterwards be manually adjusted based on visual inspection. After selection of appropriate beats, the program averages the QRST segments and the baseline into noise and artefact free 12-lead complexes. LEADS, which provides exact timing (ms) and amplitude (μV), was utilized for QRS analysis for all patients in the algorithm derivation and validation cohort. Of note, for the inter-observer agreement and to evaluate the performance of the algorithm in general clinical practice, normal print-outs of 12-lead ECGs without LEADS were used.

ECG parameters

QRS duration: QRS-onset and -offset were defined as first electrical deviation from the isoelectric line and the latest return to baseline in any of the 12 leads. In case of a slurring offset, the steepest part of the vector which returns to baseline was extended to the isoelectric line, and the offset was assigned at the crossing of these two lines. When in doubt, the vector magnitude complex containing the average of all 12-lead complexes was assessed for QRS-offset.[20]

The *S wave* in V1 was the first negative deflection following the initial R wave. The *R′ peak* in V1 was defined as the positive deflection following the S wave with the highest positive amplitude, regardless of proceeding fragmentation of the QRS complex with lower amplitude. The ratios of the time between (R′ to offset QRS)/(S to R′) and (R′ to offset QRS)/ (Q to R′) were calculated.

An *R″ deflection* in lead V1 and V2 was defined as any positive deflection in the terminal portion of the QRS after the R′ peak with the highest amplitude (*Figure 1A–C*).

In lead aVF, the *duration of the negative terminal portion of the QRS complex* (NTP) was determined as the time interval between the last change from a positive to negative deflection crossing the isoelectric line (NTP start) and the offset QRS (NTP end) (*Figure 1D–F*). The ratio of the duration of NTP/ total QRS duration was calculated.

QRS fragmentation (QRSf) was defined as an additional deflection of the QRS complex not part of the RBBB pattern in two or more contiguous leads, as previously reported.[9,22] The extent of fragmentation was determined as moderate if ≤4 leads and severe if ≥5 leads showed fragmentation.

Statistical analysis and algorithm development

Statistical analysis was first performed in the derivation cohort; the validation cohort was subsequently used for the validation of the developed diagnostic algorithm. Categorical data were reported as number with percentage and continuous data as mean with standard deviation or median with interquartile range [25th and 75th percentiles], dependent on normality of data distribution. For baseline characteristics, categorical data were compared with the chi-squared test or Fisher's exact, in accordance with the quantities per cell in the cross-table. Continuous data were assessed with the Student's *t*-test or Mann–Whitney *U* test in normally or nonnormally distributed data, respectively.

The receiver operating characteristics (ROC) curve was used to determine the optimal cut-off value of NTP (in ms) to distinguish between the presence and absence of SCAI 3, maximizing specificity over sensitivity, and the area under the curve (AUC) and its 95% confidence interval (95% CI) were reported.

Univariable logistic regression analysis was utilized to assess associations between electrocardiographic parameters and SCAI 3 (as determined by EAM/PES), and odds ratios (OR) with their respective 95% CI were reported if statistically significant. Dichotomous ECG parameters positively associated with SCAI 3 in univariable analysis were inserted into a multivariable model where variables were retained by backward stepwise selection based on the likelihood ratio.

ECG parameters independently associated with SCAI 3 were combined into a diagnostic algorithm to predict SCAI 3. Sensitivity, specificity, positive and negative predictive values of the algorithm were reported. In addition, performance of the diagnostic algorithm was assessed in the age groups
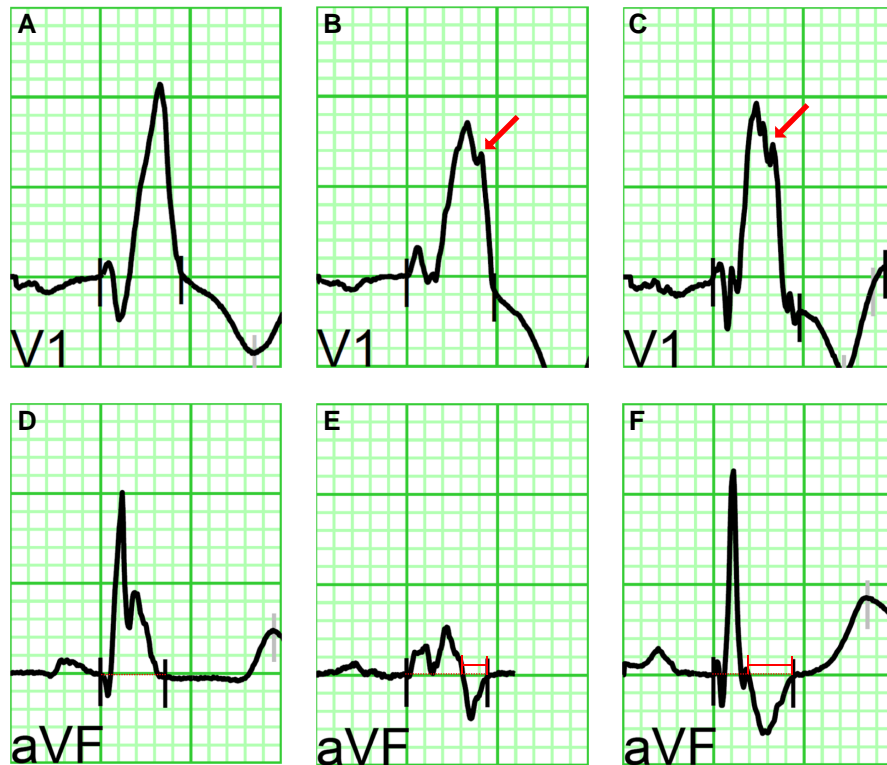
Figure 1 ECG examples. (*A–C*) Examples of QRS morphologies in lead V1. No R″ (*A*) and R″ (*B, C*) are illustrated (arrow points to R″). (*D–E*) Examples of lead aVF with the isoelectric line extended through the QRS complexes (dotted lines). The final time the QRS complex passes this line towards negative is defined as the beginning of the negative terminal portion (NTP). (*D*) Absence of NTP, in contrast to (*E*) and (*F*) where NTP is present with a duration of 54 and 100 ms, respectively (see time calliper).
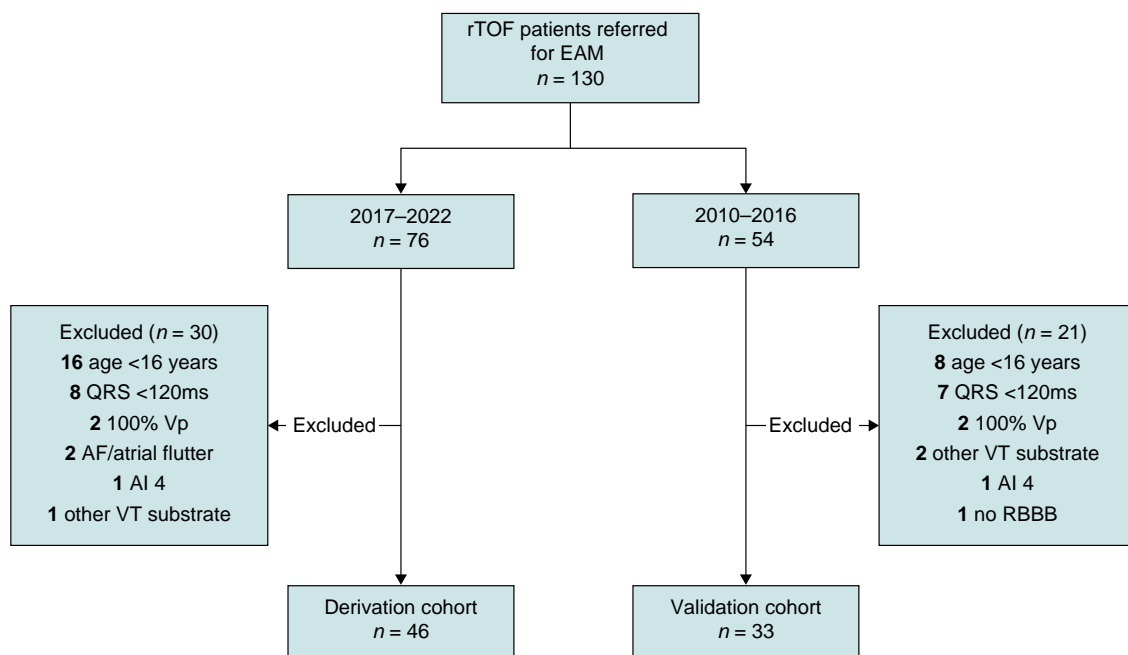

Figure 2 Flowchart of included patients. rTOF, repaired tetralogy of Fallot; EAM, electroanatomical mapping; Vp, ventricular pacing; AF, atrial fibrillation; RBBB, right bundle branch block; rest as in *Table 1*.

Table 1 Baseline table of derivation cohort

	All patients n = 46	Normal AI 3 n = 15	SCAI 3 n = 31	P-value
Age at procedure (Y)	40 ± 15	28 ± 14	46 ± 12	**0.000**
Sex (male)	32 (70%)	10 (67%)	22 (71%)	0.766
Electrophysiological study indication				
Spontaneous VT/VF	8 (17%)	–	8 (26%)	**0.038**
Before PVR	13 (28%)	7 (47%)	6 (19%)	
Risk stratification	25 (54%)	8 (53%)	17 (55%)	
Surgery				
Palliative shunt	14 (30%)	2 (13%)	12 (39%)	0.099
Age at repair (Y)	3.3 (1.2–6.6)	1.0 (0.4–1.4)	5.5 (2.8–7.0)	**0.000**
Age at repair ≥5Y	19 (44%)	2 (15%)	17 (57%)	**0.019**
TAP/RVOT patch[a]	31 (70%)	12 (80%)	19 (66%)	0.488
Transventricular repair	21 (55%)	1 (8%)	20 (80%)	**0.000**
PVR	26 (57%)	6 (40%)	20 (65%)	0.116
Age at first PVR (Y)	24 ± 14	11 ± 9	28 ± 14	**0.010**
RV-PA conduit *or* PVR <1Y after repair	4 (9%)	1 (7%)	3 (10%)	1.000
PVR >1Y after repair	25 (54%)	5 (33%)	20 (65%)	**0.047**
History				
Atrial arrhythmia	10 (23%)	1 (8%)	9 (29%)	0.237
Syncope	2 (5%)	1 (8%)	1 (3%)	0.528
Non-sustained VT	18 (46%)	5 (42%)	13 (48%)	0.708
Sustained VT/VF	9 (20%)	–	9 (29%)	**0.021**
Imaging				
Cardiac magnetic resonance				
LVEF (%)	52 ± 6	53 ± 6	52 ± 6	0.524
RVEF (%)	44 ± 7	45 ± 5	44 ± 8	0.753
RVEDV (mL)	253 ± 67	244 ± 57	259 ± 73	0.506
RVESV (mL)	141 ± 47	133 ± 36	146 ± 53	0.441
Echocardiography				
Moderate/severe LV dysfunction	1 (2%)	–	1 (3%)	1.000
Moderate/severe RV dysfunction	2 (4%)	–	2 (7%)	1.000
Moderate/severe pulmonary regurgitation	22 (48%)	9 (60%)	13 (42%)	0.250

Data are presented as number with %, median with interquartile range, or mean ± SD. P-values <0.05 are displayed in bold. AI, anatomical isthmus; LVEF/RVEF, LV/RV ejection fraction; PVR, pulmonary valve replacement; RVEDV/RVESV, RV end-diastolic/systolic volume; RVOT, RV outflow tract; RV-PA, RV to pulmonary artery; RV/LV, right/left ventricle; SCAI, slow conducting AI; TAP, transannular patch; VT/VF, ventricular tachycardia/fibrillation; Y, years.
[a]Two patients had non-transannular patch.

≥40 years and <40 years. Measurements were performed by J.W. Inter-observer agreement for the diagnostic algorithm was assessed with Cohen's kappa in the first 20 patients of the derivation cohort by a second observer (Y.K.) determining the presence or absence of the chosen ECG parameters on a standard 12-lead ECG with normal sweep speed (without LEADS). Thereafter, the algorithm was validated in the validation cohort (J.W.). Statistical analyses were performed using SPSS version 25.0 (IBM Corp., Armonk, NY). Statistical significance was defined as a P-value of <0.05.

Results

Study population

Between January 2010 and December 2022, 130 patients with rTOF were referred for EAM/PES. Distribution across the derivation and validation cohort yielded 76 and 54 patients per cohort (ratio 58:42), respectively (*Figure 2*).

Derivation cohort

In the derivation cohort, 30 patients were excluded, mainly due to age <16 years or QRS duration <120 ms, leading to a final cohort size of 46 patients. The mean age at procedure in the derivation cohort was 40 ± 15 years and 32 (70%) patients were male (*Table 1*). Indications for EAM/PES were spontaneous VA, before PVR, and for risk stratification of VA, in 8, 13, and 25 patients, respectively. The median age of patients before PVR was 23 years (18–47). Patients had repair surgery at a median age of 3.3 years (1.2–6.6), after a palliative shunt in 14 (30%), via a transventricular incision in 21 (55%) and with insertion of a TAP/RVOT patch in 31 (70%). Clinical history reported sustained VT/ventricular fibrillation in 9 (20%).

Table 2 Electrocardiographic parameters of derivation cohort

	All patients n = 46	Normal AI 3 n = 15	SCAI 3 n = 31	P-value
General Rhythm				
Sinus rhythm	43 (93%)	15 (100%)	28 (90%)	0.541
Atrial pacing	3 (7%)	–	3 (10%)	
Right bundle branch block	100%	100%	100%	–
QRS axis				
Normal	27 (59%)	11 (73%)	16 (52%)	0.065
Left	9 (20%)	–	9 (29%)	
Right	8 (17%)	4 (27%)	4 (13%)	
Extreme	2 (4%)	–	2 (7%)	
QRS duration	165 ± 23	154 ± 18	170 ± 24	**0.022**
QRS ≥150 ms	30 (65%)	6 (40%)	24 (77%)	**0.012**
QRS ≥180 ms	12 (26%)	2 (13%)	10 (32%)	0.285
QRS fragmentation	30 (65%)	9 (60%)	21 (68%)	0.605
Moderate (≤4 leads)	24 (52%)	8 (53%)	16 (52%)	0.646
Severe (≥5 leads)	6 (13%)	1 (7%)	5 (16%)	
Lead V1				
S (ms)	44 ± 6	43 ± 5	44 ± 7	0.793
R′ (ms)	114 ± 17	109 ± 17	116 ± 17	0.182
S to R′ (ms)	70 ± 17	65 ± 18	72 ± 16	0.207
S to offset QRS (ms)	121 ± 22	110 ± 19	126 ± 22	**0.020**
R′ to offset QRS (ms)	51 ± 18	45 ± 13	54 ± 19	0.100
Ratio 1 (R′ to offset QRS/S to R′)	0.71 (0.51–1.01)	0.63 (0.43–0.98)	0.73 (0.52–1.03)	0.623
Ratio 2 (R′ to offset QRS/Q to R′)	0.45 (0.32–0.58)	0.43 (0.28–0.50)	0.46 (0.33–0.65)	0.439
Presence of R″	18 (39%)	1 (7%)	17 (55%)	**0.003**
R″ (ms)	138 ± 28	87	141 ± 25	0.055
R′ to R″ (ms)	27 ± 13	15	28 ± 13	0.335
R″ to offset QRS (ms)	35 ± 18	37	35 ± 18	0.932
Lead V2				
Presence of R″	18 (39%)	6 (40%)	12 (39%)	0.933
Lead aVF				
NTP	37 (80%)	7 (47%)	30 (97%)	**0.000**
Duration of NTP	81 (59–116)	59 (38–79)	89 (68–118)	**0.029**
Duration ≥80 ms	19 (41%)	1 (7%)	18 (58%)	**0.001**
Ratio 3 (duration of NTP/QRS duration)	0.51 ± 0.20	0.38 ± 0.16	0.55 ± 0.20	0.058

NTP, negative terminal portion of the QRS complex; rest as in *Table 1*.

CMR showed a mean LV and RV ejection fraction of 52 ± 6 and 44 ± 7%, and a mean RV end-diastolic/systolic volume of 253 ± 67 and 141 ± 47 mL, respectively. Echocardiography corresponded to CMR measures indicating moderate/severely depressed LV/RV systolic function in only 1 (2%) and 2 (4%) patients, respectively (*Table 1*).

Slow conducting anatomical isthmuses

Of the 46 patients in the derivation cohort, 31 (67%) had a SCAI 3 (in 4/31 AI 3 was blocked), and 15 (33%) had a normal conducting AI 3. In addition to SCAI 3, a SCAI 2 was detected in 2 (4%) patients and none had a SCAI 1. Twenty-two monomorphic sustained ventricular tachycardias (VTs) were induced in 16 of 46 (35%) patients, of whom all had SCAI 3 as related VT substrate. The median-induced VT CL was 279 ms (240–309). Of the eight patients referred for spontaneous VA, six (75%) were inducible.

Electrocardiographic parameters and their relation to SCAI 3

The majority of patients (93%) had SR and all had an RBBB pattern on their 12-lead ECG (*Table 2*). The QRS axis was normal, left, right, and extreme, in 27 (59%), 9 (20%), 8 (17%), and 2 (4%) patients, respectively. The mean QRS duration was 165 ± 23 ms, and a QRS width of
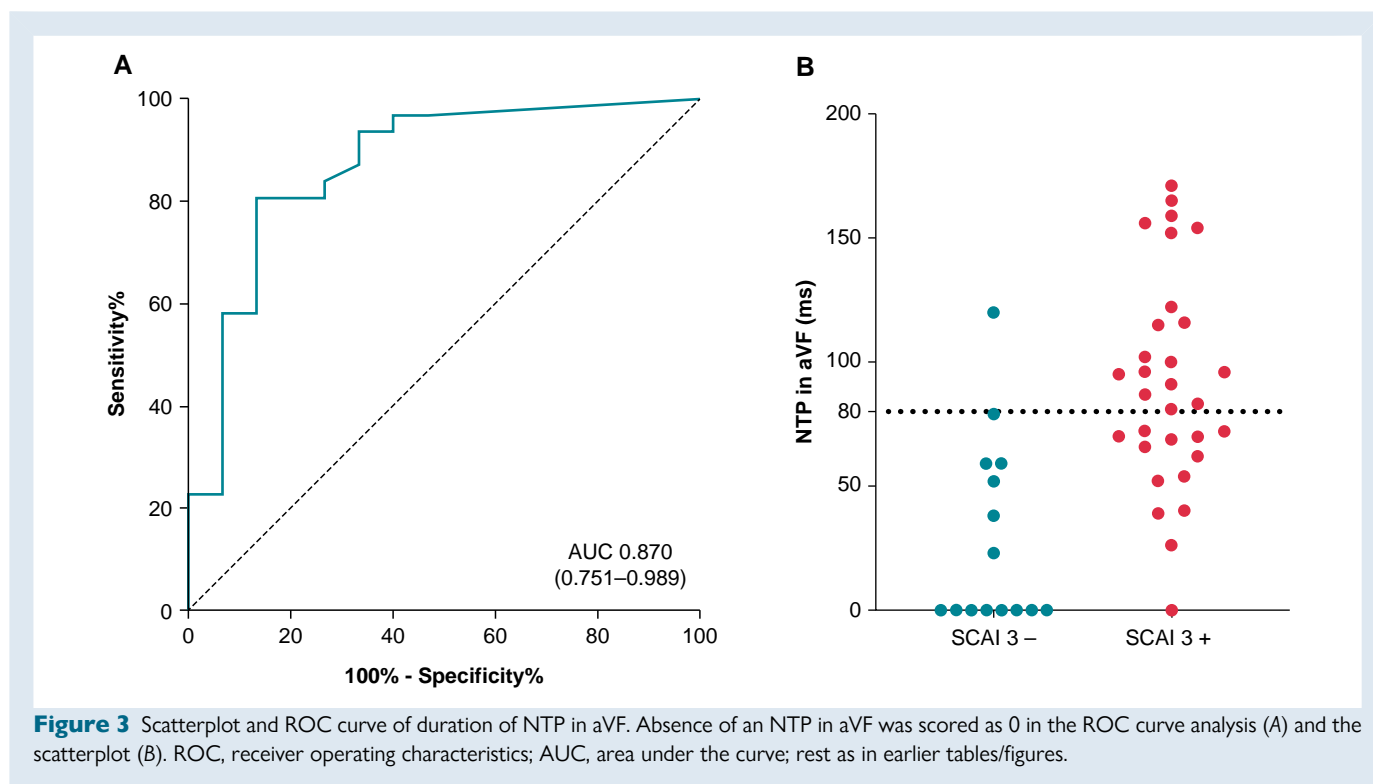
Figure 3 Scatterplot and ROC curve of duration of NTP in aVF. Absence of an NTP in aVF was scored as 0 in the ROC curve analysis (*A*) and the scatterplot (*B*). ROC, receiver operating characteristics; AUC, area under the curve; rest as in earlier tables/figures.

Table 3 Electrocardiographic parameters associated with SCAI 3 in regression analysis

Variable	OR	95% CI	P-value
Univariable analysis			
Univariable analysis			
QRS duration (per ms)	1.0	1.0–1.1	**0.030**
QRS ≥150 ms	5.1	1.4–19.5	**0.016**
S to offset QRS in V1 (per ms)	1.0	1.0–1.1	**0.029**
R″ in V1	17.0	2.0–145.7	**0.010**
NTP in aVF ≥80 ms	19.4	2.3–166.5	**0.007**
Terminal portion QRS in aVF positive	0.0	0.0–0.3	**0.002**
Multivariable analysis			
R″ in V1	10.3	1.1–97.3	**0.042**
NTP in aVF ≥80 ms	12.3	1.3–114.2	**0.028**

116). ROC curve analysis showed an overall accuracy/AUC of 0.870 (95% CI 0.751–0.989) of duration of NTP in aVF in detecting SCAI 3 with a cut-off of 61 ms (*Figure 3*). NTP ≥61 ms had the best combined sensitivity and specificity. A cut-off of NTP ≥80 ms was selected to maximize specificity over sensitivity; NTP ≥80 ms had a sensitivity of 0.58 and specificity of 0.93 for SCAI 3. Of the 19 patients with NTP in aVF ≥80 ms, 18 had SCAI 3 (95%). In 12 patients, an R″ in V1 and an NTP ≥80 ms in aVF was present simultaneously, all of whom had SCAI 3.

Table 3 provides the results of the logistic regression analysis of variables associated with SCAI 3. The parameters QRS duration (per ms), OR 1.0 (95% CI 1.0–1.1, P = 0.030), QRS ≥150 ms, OR 5.1 (95% CI 1.4–19.5, P = 0.016), S to offset QRS in V1 (per ms), OR 1.0 (95% CI 1.0–1.1, P = 0.029), R″ in V1, OR 17.0 (95% CI 2.0–145.7, P = 0.010), and NTP in aVF ≥80 ms, OR 19.4 (95% CI 2.3–166.5, P = 0.007) were all significantly associated with the occurrence of SCAI 3. Absence of an NTP in aVF (i.e. a terminal portion with a positive vector) was associated with the absence of SCAI 3: OR 0.0 (95% CI 0.0–0.3, P = 0.002). QRS ≥180 ms and R″ in V2 were not associated with SCAI 3. In multivariable logistic regression R″ in V1 (OR 10.3, 95% CI 1.1–97.3, P = 0.042) and NTP in aVF ≥80 ms (OR 12.3, 95% CI 1.3–114.2, P = 0.028) remained independently predictive of SCAI 3 (*Table 3*).

≥150 ms and QRS ≥180 ms was observed in 30 (65%) and 12 (26%), respectively. A QRS duration of ≥150 ms had a sensitivity of 77% and a specificity of 60% for SCAI 3. QRSf was present in 30 (65%), of whom 24 (52%) had moderate and 6 (13%) severe fragmentation. The sensitivity and specificity of moderate or severe QRSf for SCAI 3 was 68 and 40%, respectively.

In lead V1, the mean timing of the S wave peak was 44 ± 6 ms and of the R′ peak 114 ± 17 ms after QRS-onset, respectively. An R″ was present in 18 (39%) patients with a mean timing of 138 ± 28 ms after QRS-onset, of whom 17 of 18 (94%) had SCAI 3. In lead V2, an R″ was present in 18 (39%) patients. Lead aVF demonstrated the presence of an NTP in 37 (80%) patients with a median duration of 81 ms (59–

Diagnostic algorithm

The presence of an R″ in lead V1 and/or the duration of the NTP ≥80 ms in lead aVF were combined into a diagnostic algorithm (*Figures 4* and *5*). Seventeen of the 18 (94%) patients in the derivation cohort with an R″ in V1 had SCAI 3 and in the remaining patients without an R″ in V1 but with an NTP in aVF ≥80 ms, 6 of 7 (86%) had SCAI 3. The diagnostic algorithm had a sensitivity of 74% and a specificity of 87% for the presence of SCAI 3 with a positive and negative predictive value of 92 and 62%, respectively (*Figure 4*). Stratification for age resulted in a sensitivity and specificity of 81 and 100% in patients aged ≥40 years (n = 23) and 60 and 85% in patients aged <40 years (n = 23), respectively.
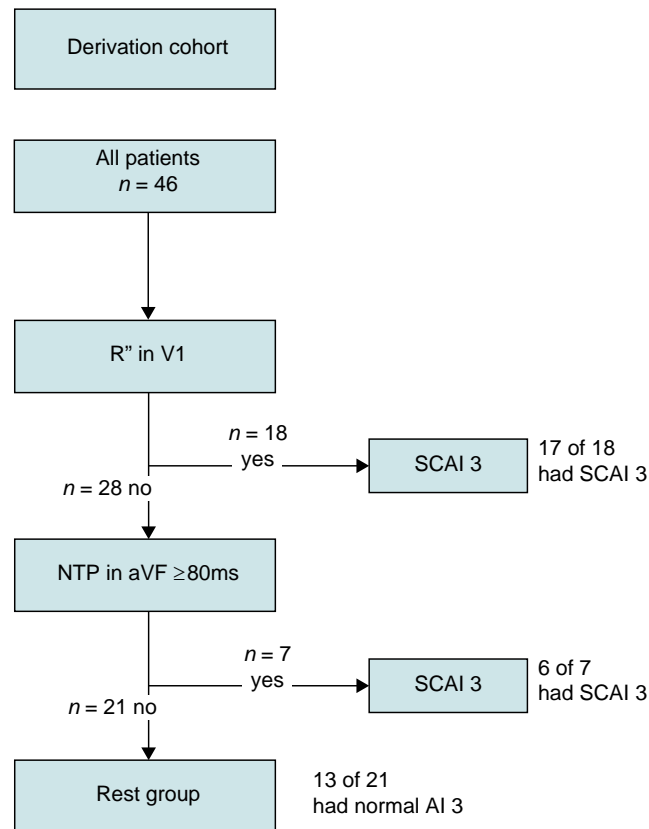
Figure 4 Diagnostic algorithm of derivation cohort.

The kappa coefficient for the inter-observer agreement was 0.900, 1.000, and 0.875, for R″ in V1, NTP ≥80 ms in aVF, and the total diagnostic algorithm, respectively.

Validation cohort

Between 2010 and 2016, 54 patients were referred for EAM/PES. Twenty-one patients were excluded from the analysis, mainly because of age <16 years or QRS duration <120 ms (*Figure 2*). The final validation cohort consisted of 33 patients (age at procedure 44 ± 15 years), of whom 18 (55%) had a SCAI 3 (4/18 with a blocked AI 3) and 15 (45%) had a normal conducting AI 3. No SCAI 1 or SCAI 2 was observed.

Thirteen of the 14 (93%) patients with an R″ in lead V1 had a SCAI 3. An NTP in aVF ≥80 ms had a sensitivity of 72% and specificity of 87% for SCAI 3. Evaluation of the diagnostic algorithm in the validation cohort resulted in a sensitivity of 83% and a specificity of 80% in predicting SCAI 3. The positive and negative predictive values were 83 and 80%, respectively (*Figure 6*).

Discussion

To the best of our knowledge this is the first study presenting the correlation between the terminal QRS vector on the 12-lead SR ECG and SCAI 3 in patients with rTOF and an RBBB pattern. Slow or absent infundibular septal conduction results in a shift of the terminal RV activation towards the lateral RVOT which leads to a late additional positive deflection (R″) in lead V1 and a prolonged terminal negative QRS vector (NTP ≥80 ms) in lead aVF. Incorporating both parameters into a

diagnostic algorithm allows for non-invasive detection of SCAI 3 with high sensitivity and specificity and excellent inter-observer agreement, which could be validated in a second cohort.

Electroanatomical basis for the terminal vector change

An RBBB pattern in TOF can occur at different levels dependent on the type of the surgical repair with a prevalence of 73% in contemporary rTOF patients.[14,22–24] Prior EAM studies have shown that global RV activation pattern and conduction velocities are similar to observed in patients with proximal RBBB, who have no structural heart disease.[12] However, local slow conduction at the septal infundibulum between the VSD patch and the pulmonary annulus (SCAI 3) significantly alters the terminal activation of the RV, with a shift in the activation wavefront from the basal lateral peri-tricuspid RV towards the lateral RVOT (*Figure 5*), provided that there is no normal conducting AI 4.[12,13] The latter is observed in only a small group of rTOF patients with a muscular ridge between the VSD patch and the tricuspid annulus, information that is usually available from the surgical reports. In these patients, rapid conduction through AI 4 will compensate for the delay through AI 3 and will result in normal terminal RV activation (*Figure 7A*). In patients without RBBB, rapid conduction through the right bundle branch leads to collision of activation wavefronts at AI 3 during SR without altering the terminal RV activation.[8,12] In very young rTOF patients, age dependent conduction, QRS axis and R wave amplitude differ from the 'adult' ECG.[25] As a consequence, patients with AI 4, narrow QRS, and very young age were excluded from the analysis.
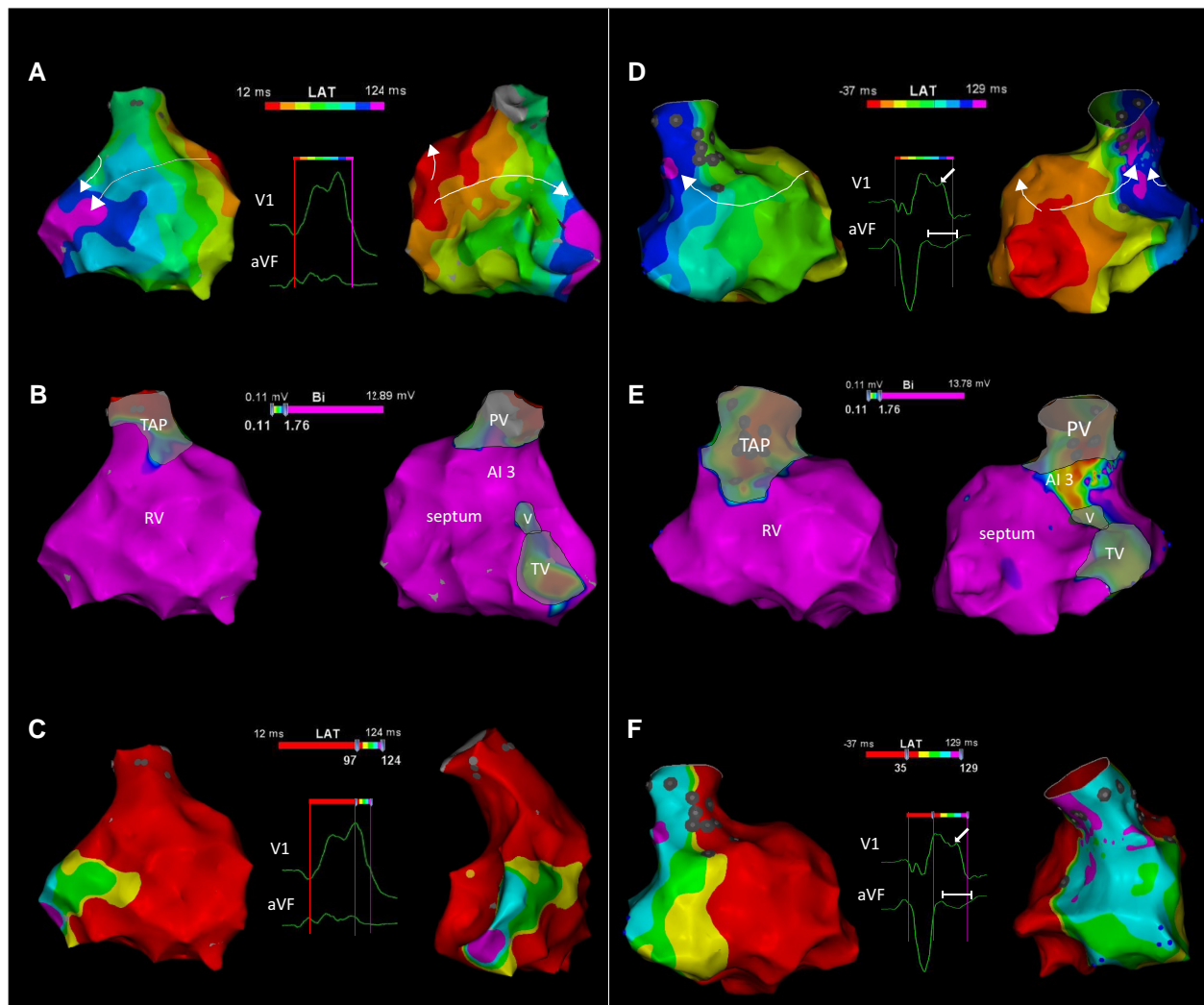
Figure 5 EAM activation and voltage mapping and correspondence with QRS characteristics. (*A*) RV activation map of a 36-year-old rTOF patient with a TAP and normal conducting AI 3. Activation times are colour-coded (8 isochrones) according to bar. The RV activation originates in the septum and the wavefront propagates over the RV free wall (left; anterior view) and through the fast conducting AI 3 (right; posterior view) with late activation of the basal lateral peri-tricuspid RV (arrows). No R″ or negative terminal deflection in aVF was observed (see inset with QRS complexes). (*B*) Bipolar voltage maps of the same patient (same views) showing high voltages at AI 3 (colour-coded according to bar). (*C*) Activation maps as in (*A*) showing the terminal activation pattern directed towards basal–lateral and inferior: activation after R′ peak in V1 is colour-coded according to five isochrones (right, modified posterior view). (*D*) RV activation maps of a 57-year-old rTOF patient with a TAP and SCAI 3 (conduction velocity 0.38 m/s). The terminal activation has shifted superiorly towards the lateral RV outflow tract leading to an R″ in V1 and a negative terminal QRS portion in aVF (inset). The views and colour-coding in (*D*), (*E*), and (*F*) as in (*A*), (*B*), and (*C*). (*E*) Bipolar voltage maps of the patient in (*D*). Note that AI 3 exhibits lower bipolar voltages and the lateral RV outflow tract (RVOT) preserved bipolar voltage. (*F*) The terminal activation is prolonged and the wavefronts are directed towards the RVOT (arrow indicates R″ in V1 and time calliper indicates NTP duration in aVF; due to baseline drifts of the Carto ECG, NTP is not optimal measurable). Recordings of the activation maps of the two patients are provided as Supplementary material online, *Videos S1 and S2*. PV/TV, pulmonary/tricuspid valve; V, VSD patch, rest as in earlier tables/figures.

In patients with SCAI 3 and in addition a SCAI 2 between a non-transannular RVOT patch and the pulmonary annulus, the terminal activation would be still directed towards the high lateral RVOT (*Figure 7B*). In patients with a SCAI 1, which is rare in our experience and not encountered in both cohorts, we would expect slow conduction through SCAI 1 and 3 with again terminal activation of the lateral RVOT (*Figure 7C*). However, in these cases we might expect that the area between the anterior RVOT/transannular patch and the anterolateral tricuspid is severely diseased and that a small late activated portion of the high lateral RVOT may not contribute to the surface ECG. However, unfortunately we do not have data to proof this assumption.

In the included rTOF patients, we hypothesized that a SCAI 3 or blocked AI 3 will lead to a terminal QRS vector with a right superior axis, which may be best reflected by a late terminal positive deflection in lead V1 and/or a negative deflection in lead aVF. Indeed, 23 of 31 (74%) patients in the derivation cohort and 15 of 18 (83%) patients in the validation cohort with a SCAI 3 had a late positive deflection R″
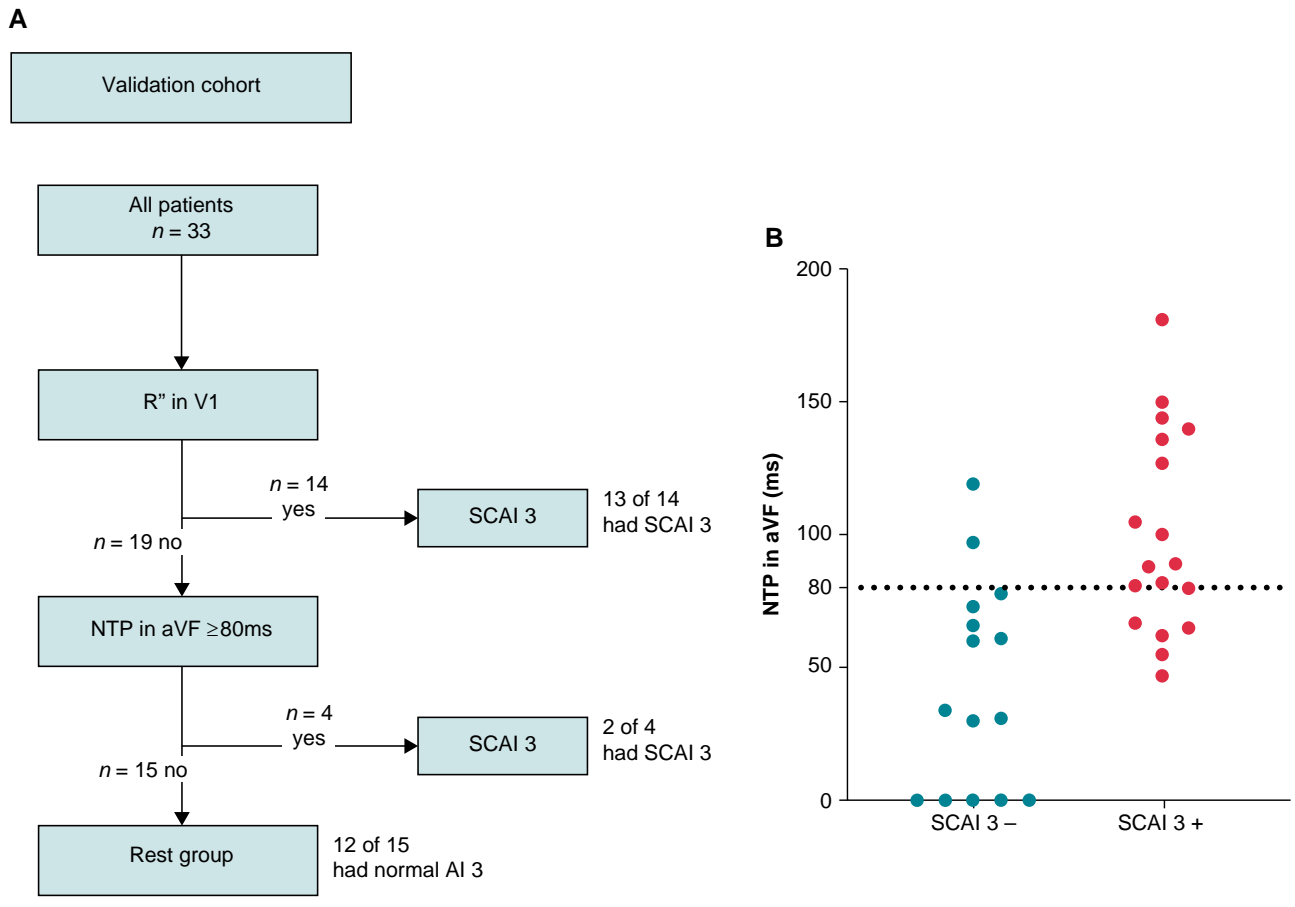
Figure 6 (*A*) Diagnostic flowchart and (*B*) scatterplot of duration of NTP stratified per presence of SCAI 3 in the validation cohort.
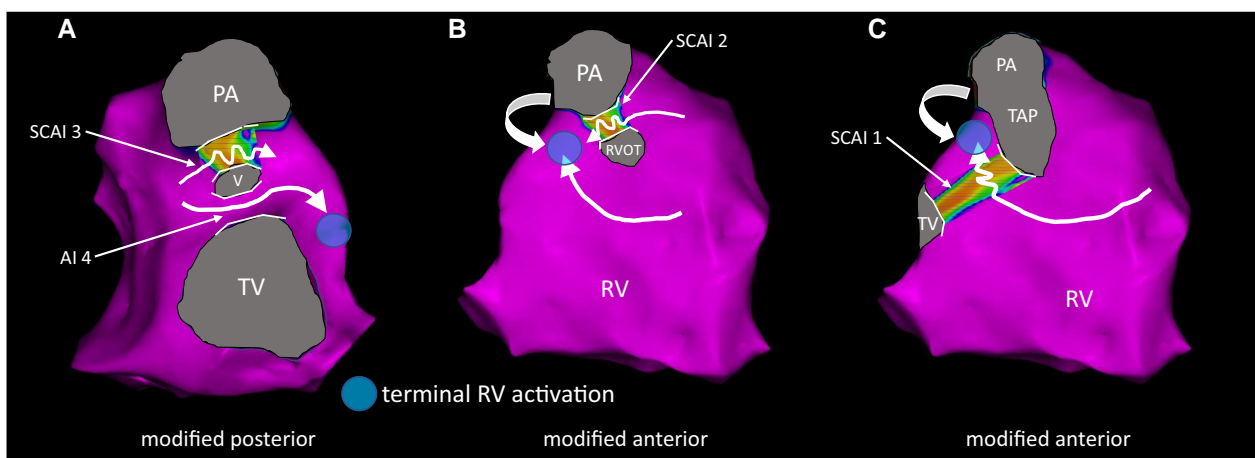

Figure 7 Expected RV activation in hypothetical scenarios. (*A–C*) Schematics of expected RV activation in hypothetical patients with SCAI 3 and an additional (slow conducting) AI. The arrows indicate the direction of RV activation, the waved arrows indicate slow conduction through a SCAI, and the circle indicates the terminal RV activation. (*A*) Simultaneous presence of a normal conducting AI 4 can counteract for the slow conduction though SCAI 3 and would lead to an RV activation similar to patients without SCAI 3. (*B*) In case of a SCAI 3 and a SCAI 2, the high lateral RVOT will remain the latest activated part of the RV (SCAI 3 not shown; RVOT indicates RVOT patch). (*C*) Similarly, the presence of SCAI 1 and SCAI 3 will lead to late activation of the lateral RVOT. Abbreviations as in earlier figures/tables.

in lead V1 and/or a broad NTP in lead aVF, which was only observed in 2 of 15 (13%) and 3 of 15 (20%) patients without SCAI, respectively.

Prior studies have reported altered RV activation in patients with rTOF.[12,15] In one series, the RV free wall was the latest activated region in 76.8% and the infundibulum in 19.6% of patients.[15] However, only global RV activation was related to total QRS duration with a weak correlation between RV activation delay and QRS.[15] Of interest, prior mapping studies performed in patients with arrhythmogenic right ventricular cardiomyopathy or right ventricular cardiac sarcoidosis have shown that RV conduction delay can significantly alter the terminal QRS, specifically in lead V1.[21,26,27]

In 26 and 17% of the patients with SCAI 3 in the derivation and validation cohort, respectively, the terminal vector of the 12-lead ECG did not reflect the electroanatomically identified activation delay. There are two important explanations for this observation. To contribute to the surface ECG, the viable mass of late activated myocardium must be large enough. Scarring in the late activated lateral RVOT with low voltages in this area can explain the lack of ECG changes. In addition, the absence of a terminal vector change in lead V1 and/or aVF may also be due to the orientation of the heart (rotation and axis) relative to the thorax.

QRS fragmentation and terminal vector alterations

In longitudinal cohort studies, the presence of QRSf, in particular if observed in several and contiguous leads, has been linked to ventricular arrhythmias, appropriate implantable cardioverter-defibrillator shocks, SCD, and all-cause mortality in patients with rTOF and other congenital heart disease.[9,22,28–31] The R″ deflection in lead V1 fulfils the criteria of QRSf but reflects more specifically, the terminal activation of the RV. In our study, an R″ deflection in lead V2 was not associated with the occurrence of SCAI 3, and in only seven patients a simultaneous R″ was observed in lead V1 and V2. The presence and extent of QRSf beyond V1 was also not associated with SCAI 3 in this study. The association between severe QRSf and VA and/or mortality may be explained by more advanced scarring of the RV and/or LV not restricted to the RVOT. Of note, QRSf was observed more frequently at the QRS-onset and in the anterior and lateral leads in congenital heart disease patients with SCD.[9] In addition, a correlation has been reported between QRSf and a decreased RV function and increased extent of RV LGE on CMR, further supporting that severe QRSf may reflect more extensive global rather than localized conduction delay in SCAI 3.[32]

Non-invasive identification of VT substrates

Non-invasive risk stratification of VT in rTOF patients remains challenging. An easy-to-use and reliable diagnostic ECG algorithm, as present for other aetiologies, is desirable.[33] One risk marker for VT and SCD has been an RBBB-like QRS prolongation ≥180 ms on the 12-lead ECG.[16] In contemporary rTOF patients, QRS duration ≥180 ms is only observed in 6–8% and the predictive value for the occurrence of VT is moderate.[1,17,22] QRS prolongation can be the consequence of SCAI or a severely enlarged RV. A prior study has suggested a QRS duration cut-off of ≥150 ms to detect SCAI or blocked AI, with however a low specificity in our study.[12] The proposed diagnostic algorithm improves the diagnostic performance of the ECG to non-invasively identify SCAI 3, which is the most important VT substrate in contemporary rTOF patients. Accordingly, the ECG algorithm may contribute to non-invasive risk stratification of VT.

Of importance, current European guidelines recommend that in patients with rTOF with sustained VT who are undergoing surgical or percutaneous PVR, pre-operative catheter mapping and transection of VT-related AIs before or during the intervention should be

considered and may be considered in those without spontaneous VTs, as AI 3 can become inaccessible after revalving.[18] The non-invasive identification of patients with SCAI 3 may help to select those patients in whom intra-operative transection can be performed without prior catheter mapping. Of importance, empirical ablation of a normal conducting and not diseased AIs may induce slow conduction, thereby creating a substrate for VT. To prevent potential harm caused by intra-operative empirical ablation in patients that may be scored as false positive with the algorithm, we preferred specificity over sensitivity in deciding the cut-off value of NTP duration for predicting SCAI 3.

Limitations

The major limitation of this study is its retrospective design and its conduction in a single tertiary referral centre. The patients referred to our expertise centre for EAM/PES may therefore not entirely reflect the general rTOF population, limiting the generalizability of the results.

The diagnostic algorithm cannot differentiate between SCAI 3 and blocked AI 3, which was observed in 8 of 49 (16%) patients with conduction block or delay across AI 3. However, in patients referred for PVR and intra-operative ablation of SCAI 3, we always perform mapping before and after cryoablation in the operation room to confirm bidirectional block. In patients with blocked AI 3, no cryoablation would be necessary. If PES and mapping are performed for risk stratification, based on previously suggested risk factors and the proposed ECG algorithm, followed by preventive ablation of SCAI 3 if present, then a small number of patients with a blocked AI 3 may not benefit from the mapping procedure. However, right ventricular mapping is not considered to increase the procedural risk of electrophysiological evaluation.

Conclusion

Terminal vectors on the 12-lead surface ECG can detect SCAI 3 in patients with rTOF and an RBBB pattern in SR. The presence of an R″ in lead V1 and/or an NTP ≥80 ms in lead aVF combine to a diagnostic algorithm with high sensitivity and specificity in predicting SCAI 3. This easy-to-use, reproducible, and low-cost method can potentially identify patients who require transection of SCAI before or during revalving and may contribute to non-invasive risk stratification for VT.

Supplementary material

Supplementary material is available at *Europace* online.

Data availability

The data underlying this article will be shared on reasonable request to the corresponding author.

References

1. Ghonim S, Gatzoulis MA, Ernst S, Li W, Moon JC, Smith GC *et al.* Predicting survival in repaired tetralogy of fallot: a lesion-specific and personalized approach. *JACC Cardiovasc Imaging* 2022;**15**:257–68.

2. Khairy P, Aboulhosn J, Gurvitz MZ, Opotowsky AR, Mongeon F-P, Kay J *et al.* Arrhythmia burden in adults with surgically repaired tetralogy of fallot: a multi-institutional study. *Circulation* 2010;**122**:868–75.

3. Silvetti MS, Bruyndonckx L, Maltret A, Gebauer R, Kwiatkowska J, Környei L *et al.* The SIDECAR project: S-IcD registry in European paediatriC and young adult patients with congenital heaRt defects. *Europace* 2023 ;**25**:460–8.

4. Engelfriet P, Boersma E, Oechslin E, Tijssen J, Gatzoulis MA, Thilén U *et al.* The spectrum of adult congenital heart disease in Europe: morbidity and mortality in a 5 year follow-up period. The Euro Heart Survey on adult congenital heart disease. *Eur Heart J* 2005;**26**:2325–33.

5. Diller GP, Kempny A, Alonso-Gonzalez R, Swan L, Uebing A, Li W *et al.* Survival prospects and circumstances of death in contemporary adult congenital heart disease patients under follow-up at a large tertiary centre. *Circulation* 2015;**132**:2118–25.

6. van der Bom T, Mulder BJM, Meijboom FJ, van Dijk APJ, Pieper PG, Vliegen HW *et al.* Contemporary survival of adults with congenital heart disease. *Heart* 2015;**101**:1989–95.

7. Koyak Z, de Groot JR, Bouma BJ, Zwinderman AH, Silversides CK, Oechslin EN *et al.* Sudden cardiac death in adult congenital heart disease: can the unpredictable be foreseen? *Europace* 2017;**19**:401–6.

8. Kapel GF, Sacher F, Dekkers OM, Watanabe M, Blom NA, Thambo JB *et al.* Arrhythmogenic anatomical isthmuses identified by electroanatomical mapping are the substrate for ventricular tachycardia in repaired tetralogy of fallot. *Eur Heart J* 2017;**38**:268–76.

9. Vehmeijer JT, Koyak Z, Bokma JP, Budts W, Harris L, Mulder BJM *et al.* Sudden cardiac death in adults with congenital heart disease: does QRS-complex fragmentation discriminate in structurally abnormal hearts? *Europace* 2018;**20**:f122–8.

10. Verstraelen TE, van Barreveld M, van Dessel PHFM, Boersma Lucas V A, Delnoy P-PPHM, Tuinenburg AE *et al.* Development and external validation of prediction models to predict implantable cardioverter-defibrillator efficacy in primary prevention of sudden cardiac death. *Europace* 2021;**23**:887–97.

11. Zeppenfeld K, Schalij MJ, Bartelings MM, Tedrow UB, Koplan BA, Soejima K *et al.* Catheter ablation of ventricular tachycardia after repair of congenital heart disease: electroanatomic identification of the critical right ventricular isthmus. *Circulation* 2007;**116**:2241–52.

12. Kapel GFL, Brouwer C, Jalal Z, Sacher F, Venlet J, Schalij MJ *et al.* Slow conducting electroanatomic isthmuses: an important link between QRS duration and ventricular tachycardia in tetralogy of fallot. *JACC Clin Electrophysiol* 2018;**4**:781–93.

13. Verzaal NJ, Masse S, Downar E, Nanthakumar K, Delhaas T, Prinzen FW. Exploring the cause of conduction delays in patients with repaired tetralogy of fallot. *Europace* 2021;**23**:i105–12.

14. Horowitz LN, Alexander JA, Edmunds L Jr. Postoperative right bundle branch block: identification of three levels of block. *Circulation* 1980;**62**:319–28.

15. Jalal Z, Sacher F, Fournier E, Cochet H, Derval N, Haissaguerre M *et al.* Right ventricular electrical activation in patients with repaired tetralogy of fallots: insights from electroanatomical mapping and high-resolution magnetic resonance imaging. *Circ Arrhythm Electrophysiol* 2019;**12**:e007141.

16. Gatzoulis MA, Till JA, Somerville J, Redington AN. Mechanoelectrical interaction in tetralogy of fallot. QRS prolongation relates to right ventricular size and predicts malignant ventricular arrhythmias and sudden death. *Circulation* 1995;**92**:231–7.

17. Possner M, Tseng SY, Alahdab F, Bokma JP, Lubert AM, Khairy P *et al.* Risk factors for mortality and ventricular tachycardia in patients with repaired tetralogy of fallot: a systematic review and meta-analysis. *Can J Cardiol* 2020;**36**:1815–25.

18. Zeppenfeld K, Tfelt-Hansen J, de Riva M, Winkel BG, Behr ER, Blom NA *et al.* 2022 ESC guidelines for the management of patients with ventricular arrhythmias and the prevention of sudden cardiac death. *Eur Heart J* 2022;**43**:3997–4126 .

19. Khairy P, Harris L, Landzberg MJ, Viswanathan S, Barlow A, Gatzoulis MA *et al.* Implantable cardioverter-defibrillators in tetralogy of fallot. *Circulation* 2008;**117**:363–70.

20. Draisma HHM SC, van der Vooren H, Maan AC, Hooft van Huysduynen B, van der Wall EE, Schalij MJ. LEADS: an interactive research oriented ECG/VCG analysis system. *Comput Cardiol* 2005; **32**:515–8.

21. Hoogendoorn JC, Venlet J, Out YNJ, Man S, Kumar S, Sramko M *et al.* The precordial R' wave: a novel discriminator between cardiac sarcoidosis and arrhythmogenic right ventricular cardiomyopathy in patients presenting with ventricular tachycardia. *Heart Rhythm* 2021;**18**:1539–47.

22. Bokma JP, Winter MM, Vehmeijer JT, Vliegen HW, van Dijk AP, van Melle JP *et al.* QRS Fragmentation is superior to QRS duration in predicting mortality in adults with tetralogy of fallot. *Heart* 2017;**103**:666–71.

23. Gelband H, Waldo AL, Kaiser GA, Bowman FO Jr, Malm JR, Hoffman BF. Etiology of right bundle-branch block in patients undergoing total correction of tetralogy of fallot. *Circulation* 1971; **44**:1022–33.

24. Horowitz LN, Simson MB, Spear JF, Josephson ME, Moore EN, Alexander JA *et al.* The mechanism of apparent right bundle branch block after transatrial repair of tetralogy of fallot. *Circulation* 1979;**59**:1241–52.

25. Dickinson DF. The normal ECG in childhood and adolescence. *Heart* 2005;**91**:1626–30.

26. Bosman LP, Cadrin-Tourigny J, Bourfiss M, Aliyari Ghasabeh M, Sharma A, Tichnell C *et al.* Diagnosing arrhythmogenic right ventricular cardiomyopathy by 2010 Task Force Criteria: clinical performance and simplified practical implementation. *Europace* 2020;**22**:787–96.

27. Lee J, Adeola O, Garan H, Stevenson WG, Yarmohammadi H. Electrocardiographic recognition of benign and malignant right ventricular arrhythmias. *Europace* 2021;**23**:1338–49.

28. Vogels RJ, Teuwen CP, Ramdjan TTTK, Evertz R, Knops P, Witsenburg M *et al.* Usefulness of fragmented QRS complexes in patients with congenital heart disease to predict ventricular tachyarrhythmias. *Am J Cardiol* 2017;**119**:126–31.

29. Egbe AC, Miranda WR, Mehra N, Ammash NM, Missula VR, Madhavan M *et al.* Role of QRS fragmentation for risk stratification in adults with tetralogy of fallot. *J Am Heart Assoc* 2018;**7**:e010274.

30. Waldmann V, Bouzeman A, Duthoit G, Koutbi L, Bessiere F, Labombarda F *et al.* Long-term follow-up of patients with tetralogy of fallot and implantable cardioverter defibrillator: the DAI-T4F nationwide registry. *Circulation* 2020;**142**:1612–22.

31. Benítez Ramos DB, Cabrera Ortega M, Castro Hevia J, Dorantes Sánchez M, Alemán Fernández AA, Castañeda Chirino O *et al.* Electrocardiographic markers of appropriate implantable cardioverter-defibrillator therapy in young people with congenital heart diseases. *Pediatr Cardiol* 2017;**38**:1663–71.

32. Park SJ, On YK, Kim JS, Park SW, Yang J-H, Jun T-G *et al.* Relation of fragmented QRS complex to right ventricular fibrosis detected by late gadolinium enhancement cardiac magnetic resonance in adults with repaired tetralogy of fallot. *Am J Cardiol* 2012;**109**:110–5.

33. El Hamriti M, Braun M, Molatta S, Imnadze G, Khalaph M, Lucas P *et al.* EASY-WPW: a novel ECG-algorithm for easy and reliable localization of manifest accessory pathways in children and adults. *Europace* 2023;**25**:600–9.